A causal and fractional all-frequency wave equation for lossy media

Sverre Holm[a)] and Sven Peter Näsholm

Department of Informatics, University of Oslo, P. O. Box 1080, NO–0316 Oslo, Norway

This work presents a lossy partial differential acoustic wave equation including fractional derivative terms. It is derived from first principles of physics (mass and momentum conservation) and an equation of state given by the fractional Zener stress-strain constitutive relation. For a derivative order α in the fractional Zener relation, the resulting absorption α_k obeys frequency power-laws as $\alpha_k \propto \omega^{1+\alpha}$ in a low-frequency regime, $\alpha_k \propto \omega^{1-\alpha/2}$ in an intermediate-frequency regime, and $\alpha_k \propto \omega^{1-\alpha}$ in a high-frequency regime. The value $\alpha = 1$ corresponds to the case of a single relaxation process. The wave equation is causal for all frequencies. In addition the sound speed does not diverge as the frequency approaches infinity. This is an improvement over a previously published wave equation building on the fractional Kelvin–Voigt constitutive relation.
© 2011 Acoustical Society of America. [DOI: 10.1121/1.3631626]

I. INTRODUCTION

This theoretical paper is concerned with lossy acoustical wave equations derived from mass and momentum conservation and constitutive relations between material stress and strain or the related pressure and density values. Such relations can be generalized by inclusion of fractional derivative orders instead of common integer derivatives.

Viscous acoustic wave absorption may be derived from the Kelvin–Voigt constitutive relation, leading to power-law frequency-dependent absorption proportional to ω^2 in the low-frequency regime, where ω denotes the angular frequency. This power-law is in accordance with what is commonly assumed in the acoustical community regarding absorption in, e.g., water and air. Above a certain frequency limit, the absorption will grow with $\sqrt{\omega}$.[1]

As compiled in Ref. [2], experimental absorption data in many different media for both compressional and shear waves follow power laws. The observed frequency dependencies sometimes follow ω^2 or $\sqrt{\omega}$, but more often the absorption grows almost linearly with frequency. This discrepancy motivates a search for wave equations, which apart from obeying the laws of mass and momentum conservation, also give rise to absorption models that agree with measurements. This has led to three different approaches to deriving wave equations. All three result in equations that include the d′Alambertian linear propagation terms $\nabla^2 u - c_0^{-2}\partial^2 u/\partial t^2$ plus some terms corresponding to absorption and dispersion combined.

For the first class, the lossless part of the wave equation is derived from a Hooke's law constitutive relation which relates stress, $\sigma(t)$, and strain, $\varepsilon(t)$: $\sigma(t) = \kappa_0^{-1}\varepsilon(t)$, where κ_0 is compressibility. The absorption part of the wave equation is derived independently and heuristically to fit experimental observations. Such approaches will not ensure that the resulting total wave equation is causal, although it may be adjusted to fulfill causality by use of Kramers–Kronig relations. Fractional derivatives in the absorption terms is a parsimonious approach to enable arbitrary frequency power laws for absorption over a wide range of frequencies. One example is the fractional Laplacian wave equation developed by Chen and Holm.[3] The existence of fractional spatial derivatives is intuitively appealing as it points to spatial properties of the medium as a possible cause of absorption. However, the wave equation is not causal as it does not model sound speed dispersion properly. This drawback was recently amended by Treeby and Cox through application of Kramers–Kronig analysis in the low-frequency regime, resulting in addition of an extra absorption term.[4] Although this class of wave equations may successfully be applied for wave propagation description and simulation, they are nevertheless derived through *ad hoc* procedures that are not directly linked to first physical principles.

The second class relies on multiple relaxation,[5] where the assumed constitutive relation for each relaxation process is a Zener model. By adjustment of the relaxation times and the compressibilities per process, the frequency-dependent absorption may then be fit to an arbitrary power-law, for example $\alpha_k \propto \omega$, which, however, becomes valid only within a certain frequency interval.[6–8] The resulting wave equation is causal. Some Zener model characteristics are considered in Sec. III A.

For the third class, the wave equation is derived from a lossy constitutive relation between stress and strain in combination with conservation laws for mass and momentum. As reviewed in Sec. II, Holm and Sinkus applied a fractional Kelvin–Voigt constitutive relation.[1] They showed that it results in power-law absorption characteristics that can model arbitrary frequency dependency, while the wave equation is causal. This is a fractional extension to the viscous absorption model. Recently, this wave equation has been extended to nonlinear acoustics.[9]

a)Author to whom correspondence should be addressed. Electronic mail: sverre@ifi.uio.no

A more detailed discussion of approaches 1 and 3 is given in Ref. 1. The developments of the present paper build on approach 3. Fractional calculus appears in a wide range of science and engineering applications, including viscoelasticity.[10] Reference 11 gives a review of the historical progress within the research on fractional calculus in solid mechanics, and Ref. 12 presents a comprehensive list of major documents and events in the area of fractional calculus up to the present date. Moreover, Mainardi has recently published a monograph that covers several aspects of the research field.[13]

This paper primarily considers the fractional Zener model for material stress-strain relations, as further discussed in Sec. III B. This paper can be regarded as an extension of the work presented in Ref. 1, where a fractional wave equation was developed based on the fractional Kelvin–Voigt model. To avoid the $c \to \infty$ artifact for $\omega \to \infty$ that arises for that model (as further explained in Sec. II), a wave equation is here instead derived from the more general fractional Zener model.

The analysis of fractional wave equations, including some based on the fractional Zener model, has previously been published with a more mathematical standpoint and notation, see e.g., Refs. 13 and 14. An additional aim of the present work is to make the acoustical research community aware of these developments as well as fitting the concepts into a framework and a notation that is more accessible to this audience. Furthermore, an intention is to shed light on various fractional stress-strain relationships described in the fields of rheology and solid mechanics and show that they may be applied to derive wave equations and the connected absorption and sound speed dispersion models by following the approaches used here. Especially results obtained in rheology, where liquid and soft solid materials are modeled, are relevant for precise description of biological matters where acoustic imaging is done.

This paper is organized as follows: Sec. II explains why both the standard and the fractional Kelvin–Voigt models give unphysical sound speed for high frequencies. Section III starts by discussing the Zener model stress-strain relation and its fractional derivative generalization as well as its relevance for viscoelastic materials. Then physical constraints on the model parameters are lined up.

Section IV presents one of the main contributions: the derivation of the fractional wave equation based on conservation of mass, conservation of momentum, and the fractional Zener model. In Sec. V, expressions for absorption and dispersion based on the fractional Zener wave equation are developed for a low-frequency regime, an intermediate regime, as well as high-frequency approximations. The three regimes present different frequency power-laws where the exponents depend on the fractional derivative order in the fractional Zener model.

II. REVIEW OF THE FRACTIONAL KELVIN–VOIGT MODEL

In Ref. 1, the fractional generalization of the Kelvin–Voigt constitutive stress-strain relation was the starting point

$$\sigma(t) = E_0\left[\varepsilon(t) + \tau_\sigma^\alpha \frac{\partial^\alpha \varepsilon(t)}{\partial t^\alpha}\right], \tag{1}$$

where E_0 is the Young's modulus at zero frequency, which equals the reciprocal of the zero-frequency compressibility κ_0. The order of the fractional derivative, α, is in the range from 0 to 2, where the standard viscous case is $\alpha = 1$. The parameter τ_σ is a time constant that characterizes the medium. The fractional Kelvin–Voigt relations was used to derive the fractional wave equation first given by Caputo[15]

$$\nabla^2 u - \frac{1}{c_0^2}\frac{\partial^2 u}{\partial t^2} + \tau_\sigma^\alpha \frac{\partial^\alpha}{\partial t^\alpha}\nabla^2 u = 0, \tag{2}$$

which has the frequency domain representation

$$k^2 - \omega^2/c_0^2 + (\tau_\sigma i\omega)^\alpha k^2 = 0. \tag{3}$$

By separation of the wavenumber k into real and imaginary parts, $k = \omega/c(\omega) - i\alpha_k$, the absorption α_k is plotted in Fig. 1 over a wide range of normalized frequency decades. The significance of the equation is that α in the range 0–0.5 gives an absorption that varies as ω^1 to $\omega^{1.5}$ in the low frequency (low $\omega \cdot \tau_\sigma$) regime. This can be used to model absorption encountered in medical ultrasound in the 1–50 MHz range. The high-frequency range can model absorption in dynamic
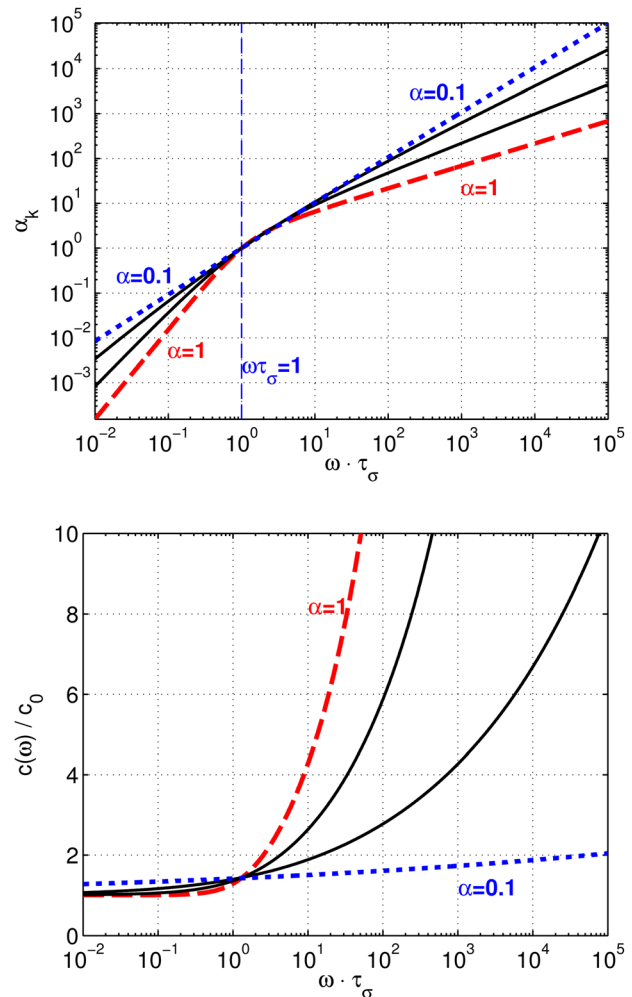

FIG. 1. (Color online) Frequency-dependent absorption (top pane) and dispersion (bottom pane), as predicted by the fractional Kelvin–Voigt model.[1] The horizontal axis represents normalized frequency. The fractional derivative order α has values 0.1, 0.3, 0.7, and 1. For visualization convenience, each absorption curve is normalized to $\alpha_k = 1$ at $\omega\tau_\sigma = 1$.

elastography, where frequencies are only in the 10–500 Hz range, but τ_σ is so much larger that $\omega \cdot \tau_\sigma \gg 1$. Asymptotically, the absorption is also in accordance with the findings of Weaver and Pao, who state that causality restricts absorption to have a slower than linear rise with frequency in the high-frequency limit.[16]

However, the corresponding phase velocity $c(\omega)$ asymptotically approaches infinity for large frequencies as illustrated in Fig. 1. This effect is also predicted directly from the constitutive relation [Eq. (1)], which has the frequency domain representation

$$\sigma(\omega) = E_0[1 + (\tau_\sigma i\omega)^\alpha]\varepsilon(\omega), \tag{4}$$

which for high $\omega\tau_\sigma$ becomes $\sigma(\omega) \approx E_0(\tau_\sigma i\omega)^\alpha \varepsilon(\omega)$. With increased frequency, there is thus a growing coupling between strain and stress, implying that a sudden change in stress is felt instantaneously all over the medium. This was pointed out in the geophysics literature a long time ago for the non-fractional Kelvin-Voigt stress-strain relation.[17] Meidav suggested that by using the more general Zener model, this problem may be avoided.[18] This preferred high frequency behavior motivates why the wave equation derived and analyzed in the present paper is based on the more general fractional Zener model.

III. STRESS-STRAIN CONSTITUTIVE RELATIONS

A. The Zener model

The Zener model, sometimes denoted the Standard Linear Solid model or the Standard Viscoelastic Body, describes the following constitutive strain-stress relation, presented by Zener for metals[19]

$$\sigma(t) + \tau_\varepsilon \frac{\partial \sigma(t)}{\partial t} = E_0\left[\varepsilon(t) + \tau_\sigma \frac{\partial \varepsilon(t)}{\partial t}\right]. \tag{5}$$

The parameter $\tau_\sigma = \eta/E_0$ is the creep or retardation time, where η is the viscosity. The relaxation time is denoted τ_ε. See also the next section where an account is given of physical constraints on the physical parameters. For the case $\tau_\varepsilon = 0$, the Zener model equals the Kelvin–Voigt model. The use of mechanical analogs for the acoustics of fluids was also treated in Ref. 20, where the Maxwell model, the Kelvin–Voigt model (there denoted the Stokes model), and the combination of them as the Zener model of Eq. (5) were investigated.

B. The fractional Zener model generalization

Fractional constitutive stress-strain relations have been studied in mechanical engineering for several decades. In comprehensive review papers,[21,22] Rossikhin and Shitikova summarize research on fractional calculus in dynamic problems of solid mechanics. The reviews analyze a comprehensive number of constitutive relations, of which the fractional Kelvin–Voigt model and the more general fractional Zener model are among the more straightforward.

In the following is a representation of a fractional Zener model similar to the formulation introduced by Bagley and Torvik in Eq. (3) of Ref. 23:

$$\sigma(t) + \tau_\varepsilon^\beta \frac{\partial^\beta \sigma(t)}{\partial t^\beta} = E_0\left[\varepsilon(t) + \tau_\sigma^\alpha \frac{\partial^\alpha \varepsilon(t)}{\partial t^\alpha}\right]. \tag{6}$$

In this paper, it is assumed that the that the medium is isotropic so that the time constants, the Young's modulus, and the fractional derivative orders are direction independent.

Parameter fits to experimental measurements indicate that this model is applicable to a wide range of materials, e.g., arterial viscoelasticity,[24] brain,[25–28] doped corning glass,[23] rock,[18] liver,[27] metals,[29] polymeric materials,[30–33] and rubber.[34]

It should be noted that even more general fractional stress-strain relations may be used to describe material response, as stated in, e.g., Ref. 22. One example is the five-parameter approach described in Ref. 35. This and other generalized models could equally well be applied in the wave equation derivations in the following text.

The stress-strain relation model used in Ref. 23, which has a structure corresponding to Eq. (6) here, is further analyzed in Ref. 34. There, constraints on the model parameters are derived based on thermodynamic considerations founded on the principle of nonnegative rate of energy dissipation and on a nonnegative internal work. Converting the parameters in the stress-strain relation of Bagley and Torvik into the format of Eq. (6) results in the constraints that $E_0 \geq 0$ and $\tau_\sigma^\alpha \geq \tau_\varepsilon^\beta > 0$. They also argue that to get a monotonically decreasing stress relaxation function for positive time, the fractional derivative orders must be equal, $\alpha = \beta$. A slightly looser criterion is to require that the stress relaxation function only should be asymptotically monotonic; in this case, it is sufficient with $\alpha \geq \beta$.[36] Based on these arguments the subsequent discussion in this paper will mainly treat situations when $\alpha = \beta$.

IV. WAVE EQUATION, DISPERSION RELATION, AND COMPRESSIBILITY DERIVATIONS

A. A fractional Zener wave equation

In the following is a deduction of a wave equation based on the fractional Zener model of Eq. (6). Due to the conservation of mass principle, strain is related to displacement in isotropic media by

$$\varepsilon(t) = \nabla u(t) \overset{\mathscr{F}}{\longleftrightarrow} \varepsilon(\omega) = -iku(\omega), \tag{7}$$

where $u(t)$ is the displacement vector. The right-hand side of the expression is the Fourier-domain formulation, which is for assuming a harmonic plane wave $u = \exp[i(\omega t - kx)]$, where the wavenumber vector is k, the angular frequency ω, and x the spatial coordinate vector.

Insertion of $\varepsilon(t)$ from Eq. (7) into the Zener model [Eq. (6)] and application of the ∇ operator on both sides gives

$$\left[1 + \tau_\varepsilon^\beta \frac{\partial^\beta}{\partial t^\beta}\right]\nabla\sigma(t) = E_0\left[1 + \tau_\sigma^\alpha \frac{\partial^\alpha}{\partial t^\alpha}\right]\nabla^2 u(t). \tag{8}$$

Furthermore, following the principle of conservation of momentum, Newton's second law may be formulated as

$$\nabla\sigma(t) = \rho\frac{\partial^2 u(t)}{\partial t^2} \overset{\mathscr{F}}{\longleftrightarrow} -ik\sigma(\omega) = \rho(i\omega)^2 u(\omega), \tag{9}$$

where ρ denotes the medium density. Insertion of the relation for the spatial derivative of $\sigma(t)$ into Eq. (8), and the sound speed definition $c_0^2 \overset{\Delta}{=} 1/(\rho\kappa_0) = E_0/\rho$, then leads to the fractional Zener model wave equation

$$\nabla^2 u - \frac{1}{c_0^2}\frac{\partial^2 u}{\partial t^2} + \tau_\sigma^\alpha \frac{\partial^\alpha}{\partial t^\alpha}\nabla^2 u - \frac{\tau_\varepsilon^\beta}{c_0^2}\frac{\partial^{\beta+2} u}{\partial t^{\beta+2}} = 0. \quad (10)$$

The two final terms are the loss terms, which will be interpreted in terms of their effect on absorption and sound speed dispersion. The first one contains a second order spatial derivative and a fractional time derivative, whereas the second term contains a higher order fractional time derivative. This wave equation is also a generalization of the fractional wave equation of Eq. (2), which is obtained by setting $\tau_\varepsilon = 0$. A 1-D medium will be assumed subsequently without loss of generality, so from now on k is a scalar wavenumber.

B. Fractional Zener model dispersion relation and compressibility

The frequency-domain representation of the fractional Zener model [Eq. (6)] is

$$\left[1 + (\tau_\varepsilon i\omega)^\beta\right]\sigma(\omega) = E_0[1 + (\tau_\sigma i\omega)^\alpha]\varepsilon(\omega). \quad (11)$$

Substitution of $\varepsilon(\omega)$ in the preceding equation by use of Eq. (7), solving the result for $\sigma(\omega)$, and insertion of the result into Eq. (9) leads to

$$\rho(i\omega)^2 u(\omega) = -ikE_0\frac{1 + (\tau_\sigma i\omega)^\alpha}{1 + (\tau_\varepsilon i\omega)^\beta}(-iku(\omega)), \quad (12)$$

which can be solved to give a dispersion relation between k and ω

$$k^2 = \frac{\omega^2}{c_0^2}\frac{1 + (\tau_\varepsilon i\omega)^\beta}{1 + (\tau_\sigma i\omega)^\alpha}. \quad (13)$$

Note that when $\tau_\varepsilon = 0$, the fractional Zener model dispersion relation [Eq. (13)] equals the fractional Kelvin–Voigt model dispersion relation [Eq. (3)]. From Eq. (11), the compressibility $\kappa(\omega) \overset{\Delta}{=} \varepsilon(\omega)/\sigma(\omega)$ may be expressed as

$$\kappa(\omega) = \frac{1}{E_0}\frac{1 + (\tau_\varepsilon i\omega)^\beta}{1 + (\tau_\sigma i\omega)^\alpha} = \kappa_0\frac{1 + (\tau_\varepsilon i\omega)^\beta}{1 + (\tau_\sigma i\omega)^\alpha}, \quad (14)$$

which leads to a common expression for dispersion

$$k^2 - \rho\kappa(\omega)\omega^2 = 0. \quad (15)$$

V. FRACTIONAL ZENER ABSORPTION AND DISPERSION

The frequency dependency of the sound speed $c(\omega)$ (dispersion) and the absorption α_k may be extracted from the real and imaginary parts of the complex wavenumber

$$k = \frac{\omega}{c(\omega)} - i\alpha_k. \quad (16)$$

The wavenumber k may be solved from the dispersion relation, Eq. (13), by taking the square root and identifying the imaginary and real parts. This gives $\alpha_k(\omega)$ and $c(\omega)$, which is interpreted in the following text in terms of asymptotic values in three distinct frequency regimes.

Absorption and dispersion plots in the low- and high-frequency regimes are seen in Figs. 2 and 3 where $\tau_\sigma/\tau_\varepsilon = 10$ for a set of values of $\alpha = \beta$ between 0.1 and 1. Note that the range is restricted to 0.1 because the equations derived here have an anomaly as α approaches 0. As discussed in Ref. 1, this problem may be avoided by taking the limit as α approaches 0. The intermediate regime covers a greater frequency region as the ratio increases as may be confirmed for the $\tau_\sigma/\tau_\varepsilon = 1000$ case.

The break-points between the three different frequency regimes of Eq. (13) are determined by the relation between $(\omega\tau_\varepsilon)^\beta$ and $(\omega\tau_\sigma)^\alpha$. These regimes are denoted in the following text as the low-, intermediate-, and high-frequency regimes. Because the time constants τ_ε and τ_σ are material-dependent, the frequency intervals relevant for the respective regimes differ between media.
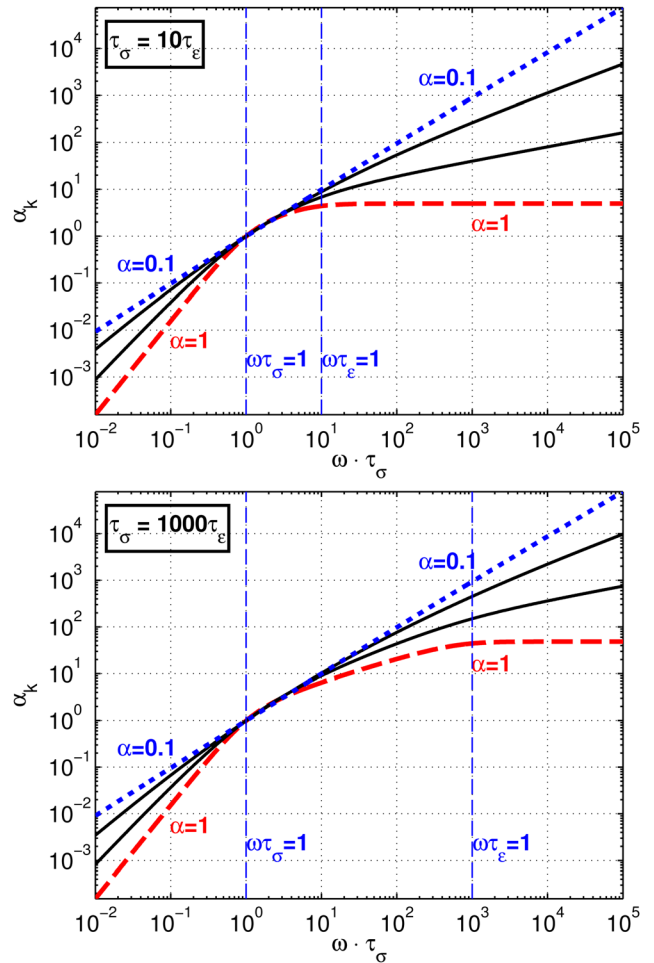

FIG. 2. (Color online) Frequency-dependent absorption for $\tau_\sigma = 10\tau_\varepsilon$ (top pane) and $\tau_\sigma = 1000\tau_\varepsilon$ (bottom pane) as predicted by the fractional Zener model by taking the negative imaginary part of k calculated from Eq. (13). The horizontal axis represents normalized frequency. The fractional derivative order α has values 0.1, 0.3, 0.7, and 1. For visualization convenience, each absorption curve is normalized to $\alpha_k = 1$ at $\omega\tau_\sigma = 1$.
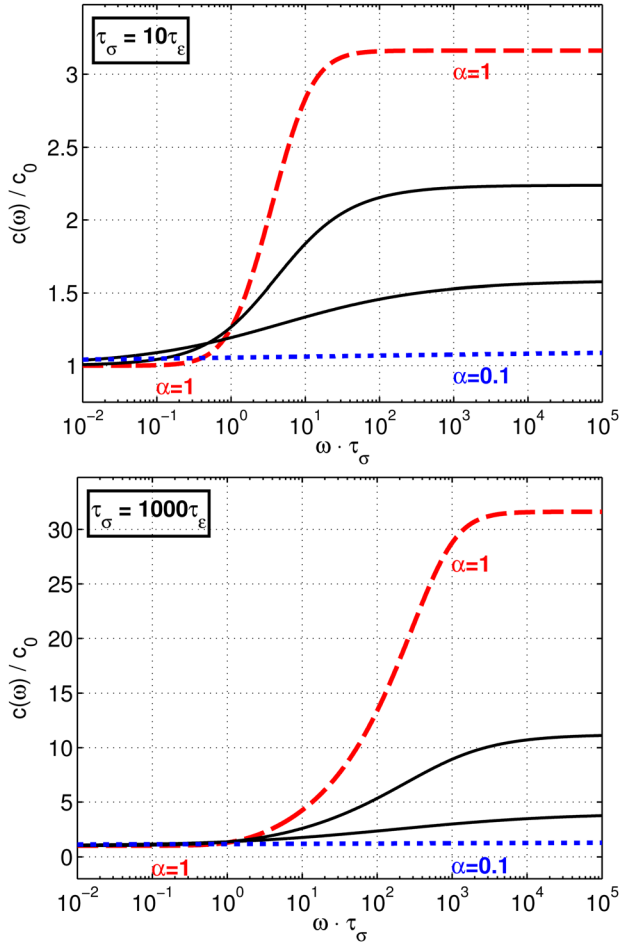
FIG. 3. (Color online) Normalized frequency-dependent sound speed for $\tau_\sigma = 10\tau_\varepsilon$ (top pane) and $\tau_\sigma = 1000\tau_\varepsilon$ (bottom pane) as predicted by the fractional Zener model by taking the real part of k calculated from Eq. (13). The horizontal axis represents normalized frequency. The fractional derivative order α has values 0.1, 0.3, 0.7, and 1.

A. The low-frequency regime $(\omega\tau_\varepsilon)^\beta \ll 1, (\omega\tau_\sigma)^\alpha \ll 1$

In the low-frequency interval where $(\omega\tau_\varepsilon)^\beta \ll 1$ and $(\omega\tau_\sigma)^\alpha \ll 1$, the complex wavenumber may be approximated by

$$k \approx \frac{\omega}{c_0}\left[1 + \frac{1}{2}(\tau_\varepsilon i\omega)^\beta\right]\left[1 - \frac{1}{2}(\tau_\sigma i\omega)^\alpha\right]$$
$$\approx \frac{\omega}{c_0}\left[1 - \frac{1}{2}\left((\tau_\sigma i\omega)^\alpha - (\tau_\varepsilon i\omega)^\beta\right)\right]. \qquad (17)$$

For $\alpha = \beta$, the wavenumber then becomes

$$k \approx \frac{\omega}{c_0}\left[1 - \frac{1}{2}\left(\tau_\sigma^\alpha - \tau_\varepsilon^\alpha\right)(i\omega)^\alpha\right]. \qquad (18)$$

Utilizing the relation $i^\alpha = \cos(\pi\alpha/2) + i\sin(\pi\alpha/2)$ therefore gives the absorption

$$\alpha_k(\omega) = -\Im m\, k \approx \frac{\omega^{1+\alpha}}{2c_0}\left(\tau_\sigma^\alpha - \tau_\varepsilon^\alpha\right)\sin\frac{\pi\alpha}{2}, \qquad (19)$$

which is proportional to $\omega^{1+\alpha}$ as exemplified in the top pane part of Fig. 2. The real part of Eq. (18) similarly gives the dispersion

$$\Re e\, k \approx \frac{\omega}{c_0}\left[1 - \frac{(\omega\tau_\sigma)^\alpha - (\omega\tau_\varepsilon)^\alpha}{2}\cos\frac{\pi\alpha}{2}\right]. \qquad (20)$$

As illustrated in Fig. 3, the sound speed $c(\omega)$ is therefore constant for very low frequencies.

B. The intermediate- frequency regime $(\omega\tau_\varepsilon)^\beta \ll 1 \ll (\omega\tau_\sigma)^\alpha$

The intermediate- frequency regime is distinguished by $(\omega\tau_\varepsilon)^\beta \ll 1 \ll (\omega\tau_\sigma)^\alpha$. Assuming that $\alpha = \beta$ and rewriting Eq. (13) to

$$k^2 = \left(\frac{\omega}{c_0}\right)^2\left(\frac{1}{\tau_\sigma i\omega}\right)^\alpha \frac{1 + (\tau_\varepsilon i\omega)^\alpha}{1 + (\tau_\sigma i\omega)^{-\alpha}}, \qquad (21)$$

then allows for approximating the wavenumber to

$$k \approx \frac{\omega^{1-\alpha/2}(\tau_\sigma i)^{-\alpha/2}}{c_0}\left[1 + \frac{1}{2}(\tau_\varepsilon i\omega)^\alpha\right]\left[1 - \frac{1}{2}(\tau_\sigma i\omega)^{-\alpha}\right]. \qquad (22)$$

Because both $(\tau_\sigma i\omega)^{-\alpha}$ and $(\tau_\varepsilon i\omega)^\alpha$ are small in the intermediate regime, k may further be approximated to

$$k \approx \frac{\omega^{1-\alpha/2}(\tau_\sigma i)^{-\alpha/2}}{c_0} \cdot \left[1 - \frac{1}{4}\left[\frac{\tau_\varepsilon}{\tau_\sigma}\right]^\alpha\right]. \qquad (23)$$

The imaginary part of this gives the absorption coefficient

$$\alpha_k(\omega) \approx \frac{\tau_\sigma^{-\alpha/2}}{c_0}\sin\frac{\pi\alpha}{4}\left[1 - \frac{1}{4}\left[\frac{\tau_\varepsilon}{\tau_\sigma}\right]^\alpha\right]\omega^{1-\alpha/2}. \qquad (24)$$

In Fig. 3, where $\tau_\sigma = 1000\tau_\varepsilon$, the intermediate regime approximation is valid in the normalized-frequency interval $\tau_\sigma\omega \in [10^0, 10^3]$.

The absorption described by Eq. (24) is proportional to $\omega^{1-\alpha/2}$. This is equal to the high-frequency asymptote of the absorption resulting from the fractional Kelvin–Voigt dispersion relation [Eq. (3)], as developed in Ref. 1. Actually, the viscous absorption described by the Kelvin–Voigt and the fractional Kelvin–Voigt equations may thus be interpreted as the intermediate regime of the fractional Zener model being extended to very large frequencies without the high-frequency regime described in the next section.

The intermediate regime frequency-dependent sound speed given by the wavenumber approximation [Eq. (23)] is

$$c(\omega) \approx \frac{\omega}{\Re e\, k} \approx c_0\frac{\tau_\sigma^{\alpha/2}}{\cos(\pi\alpha/4)}\left[1 - \frac{1}{4}\left[\frac{\tau_\varepsilon}{\tau_\sigma}\right]^\alpha\right]^{-1}\omega^{\alpha/2}, \quad (25)$$

as exemplified in the top pane of Fig. 3 for $\omega\tau_\sigma \in [10^0, 10^1]$ and in the bottom pane of Fig. 3 for $\omega\tau_\sigma \in [10^0, 10^3]$.

C. The high-frequency regime $(\omega\tau_\varepsilon)^\beta \gg 1, (\omega\tau_\sigma)^\alpha \gg 1$

The high-frequency regime is distinguished by $(\omega\tau_\varepsilon)^\beta \gg 1$ and $(\omega\tau_\sigma)^\alpha \gg 1$. Assuming that $\alpha = \beta$, and rewriting Eq. (13) to

$$k^2 = \left(\frac{\omega}{c_0}\right)^2 \left(\frac{\tau_\varepsilon}{\tau_\sigma}\right)^\alpha \frac{1 + (\tau_\varepsilon i\omega)^{-\alpha}}{1 + (\tau_\varepsilon i\omega)^{-\alpha}}, \quad (26)$$

gives the wavenumber approximation

$$k \approx \frac{\omega}{c_0} \left(\frac{\tau_\varepsilon}{\tau_\sigma}\right)^{\alpha/2} \left[1 + \frac{1}{2}(\tau_\varepsilon i\omega)^{-\alpha}\right] \left[1 - \frac{1}{2}(\tau_\sigma i\omega)^{-\alpha}\right]$$
$$\approx \frac{\omega}{c_0} \left(\frac{\tau_\varepsilon}{\tau_\sigma}\right)^{\alpha/2} \left[1 + \frac{(i\omega)^{-\alpha}}{2}\left(\tau_\varepsilon^{-\alpha} - \tau_\sigma^{-\alpha}\right)\right]. \quad (27)$$

The negative imaginary part gives the absorption

$$\alpha_k(\omega) \approx \left(\frac{\tau_\varepsilon}{\tau_\sigma}\right)^{\alpha/2} \sin(\pi\alpha/2) \frac{\tau_\varepsilon^{-\alpha} - \tau_\sigma^{-\alpha}}{2c_0} \omega^{1-\alpha}, \quad (28)$$

as illustrated in the right-hand asymptotes of Fig. 2, while the sound-speed dispersion is given from Eq. (27) by $c(\omega) = \omega/\mathfrak{Re}\,k$. The sound speed becomes frequency-independent for very high frequencies:

$$c = c_0(\tau_\sigma/\tau_\varepsilon)^{\alpha/2}, \quad (29)$$

which is greater than c_0 because $\tau_\sigma > \tau_\varepsilon$, as put forward in Sec. III B. The sound speed frequency-dependency is illustrated in Fig. 3.

D. Wave equation causality

Wave equation (10) has been found from the physical principles of conservation of mass and momentum in combination with a constitutive equation and this should be enough to ensure that it is causal. It can be verified by observing that the frequency-domain compressibility as given in Eq. (14) through the inverse Fourier transform gives a causal time-domain compressibility:

$$\kappa(t) = \frac{\kappa_0 t^{\alpha-1}}{\tau_\sigma^\alpha} H(t)\Big[E_{\alpha,\alpha}(-(t/\tau_\sigma)^\alpha)$$
$$+ (\tau_\varepsilon/t)^\beta E_{\alpha,\alpha-\beta}(-(t/\tau_\sigma)^\alpha)\Big], \quad (30)$$

where $H(t)$ is the Heaviside step function and $E_{a,b}(t)$ here denotes the two-parameter Mittag–Leffler function, which may be regarded as a generalization of the exponential function. Its one-sided Laplace transform is given in Ref. 37, from which the Fourier transform can be deduced.

In addition, by following the pattern of Kramers–Kronig analysis in, e.g., Ref. 38 while choosing appropriate subtraction frequencies, causality for the low-, intermediate-, and high-frequency regimes may be proven.

VI. DISCUSSION AND CONCLUDING REMARKS

The fractional derivative description of the loss terms in the wave equation can be considered as a special case of a general convolution operator. An advantage of the fractional derivative is that its Fourier transforms give power-law functions. For wave equations, this is consistent with power-law

absorption. Therefore one gets a description with fewer parameters that may be considered as more parsimonious than alternative approaches.

The acoustic wave equation derived in this paper has several desirable properties. First, it is based only on first principles of physics (mass conservation and momentum conservation) and the fractional Zener stress-strain relation. This relation is a constitutive equation experimentally shown to be valid for a wide range of materials.

Second, it is causal for any frequency. There is thus no need for *ad hoc* addition of some extra term to fulfill the Kramers–Kronig relation.

Third, the attenuation follows a frequency power-law $\alpha_k(\omega) = \alpha_0\omega^y$, with different y and α_0 in the distinct low-frequency, intermediate-frequency, and high-frequency regimes.

Fourth, the high-frequency asymptote of the sound speed is physical in the sense that it does not grow to infinity with increasing frequency.

Fifth, the model can be considered to be a fractional generalization of a single relaxation model, frequently used for describing attenuation and dispersion in gases and liquids.[5] This can also be seen in Fig. I-4 of Ref. 20; this figure is comparable to our figures for $\alpha = 1$. In air, the two main relaxation processes are due to nitrogen and oxygen.[39] As an example the oxygen component at 0% relative humidity, 20 °C and 1 atm causes a sound speed increase from 343.23 to 343.35 m/s in the transition region between 10 and 100 Hz.[40] According to Eq. (29), this is equivalent to a ratio $\tau_\sigma/\tau_\varepsilon \approx 1.0007$. Another example is fluorine where the speed of sound changes from 332 to 339 m/s between 5 and 200 kHz at 102 °C and 1 atm,[41] resulting in $\tau_\sigma/\tau_\varepsilon \approx 1.043$. In the examples given here, we have on purpose exaggerated this ratio as also done in Ref. 18. Otherwise the transition region would not have been visible. Likewise, one usually refers to the low-frequency attenuation as being proportional to ω^2, and the high-frequency region as having constant attenuation for the single relaxation process, as the transition region is so narrow that it can be neglected.

In addition to applications in modeling of medical ultrasound as discussed in Sec. II, another area where the presented work may be significant is elastography where tissue is excited by shear waves in the frequency range where the Kelvin–Voigt stress-strain relation is valid.[42,43] Dynamic elastography typically falls in the intermediate-frequency region discussed here. However, if the frequencies in these applications were pushed up to the regime where the Kelvin–Voigt model is no longer valid, i.e., for $(\omega\tau_\varepsilon)^\beta > 1$, the modeling presented in the present work could make tissue classification more accurate.

Another field where accurate frequency-dependent absorption and sound speed models are required to avoid image distortion is photoacoustic imaging and tomography, where laser pulses transmit into tissue interact to produce ultrasound emission that is detected to form images.[44] Similarly, the accuracy of radiation force imaging of sound speed dispersion depends on reliable tissue models.[45,46]

In second-order ultrasound field (SURF) imaging, transmit pulses consist of an elasticity-manipulating low-

frequency component in conjunction with a high-frequency acoustic imaging component. The elasticity manipulation is due to the medium nonlinearity. SURF imaging may be utilized to, e.g., improve microbubble contrast agent imaging,[47] suppress reverberations,[48] and estimate local material nonlinearity.[49] The total bandwidth of a SURF pulse complex is wide. Therefore numerical propagation-simulation with such pulses in lossy media could be more precise if the fractional Zener all-frequency attenuation- and sound speed dispersion model combined with nonlinear acoustics[9] is employed.

This paper presents little theoretical justification for why fractional derivatives occur in the constitutive models. However, there are papers which motivate their relevance from a statistical point of view. Papoulia *et al.* have shown that rheological representations like a generalized Zener model where the number of springs/dashpots tends to infinity, converge to a corresponding fractional model.[50] Adolfsson *et al.* have demonstrated both numerically and analytically that a large number of internal variables each representing a specific damping mechanism converges to a fractional model with a single internal variable.[51] Chatterjee has presented examples where viscoelastic damping due to several simultaneously decaying processes with closely spaced exponential decay rates are shown to induce a constitutive behavior involving fractional order derivatives.[52] Machado and Galhano have shown that averaging over a large population of microelements, each having integer-order nature, gives global dynamics with both integer and fractional dynamics.[53] Work is also under way to relate the new model of this paper to the established multiple relaxation model of Ref. 5.

ACKNOWLEDGMENTS

[1] S. Holm and R. Sinkus, "A unifying fractional wave equation for compressional and shear waves," J. Acoust. Soc. Am. **127**, 542–548 (2010).

[2] T. Szabo and J. Wu, "A model for longitudinal and shear wave propagation in viscoelastic media," J. Acoust. Soc. Am. **107**, 2437–2446 (2000).

[3] W. Chen and S. Holm, "Fractional Laplacian time-space models for linear and nonlinear lossy media exhibiting arbitrary frequency power-law dependency," J. Acoust. Soc. Am. **115**, 1424–1430 (2004).

[4] B. Treeby and B. Cox, "Modeling power law absorption and dispersion for acoustic propagation using the fractional Laplacian," J. Acoust. Soc. Am. **127**, 2741–2748 (2010).

[5] A. I. Nachman, J. F. Smith III, and R. C. Waag, "An equation for acoustic propagation in inhomogeneous media with relaxation losses," J. Acoust. Soc. Am. **88**, 1584–1595 (1990).

[6] B. A. J. Angelsen, *Ultrasound Imaging. Waves, Signals and Signal Processing*, (Emantec, Trondheim, Norway, 2000), Vol. 1, Chap. 4.6E.

[7] M. Tabei, T. D. Mast, and R. C. Waag, "Simulation of ultrasonic focus aberration and correction through human tissue," J. Acoust. Soc. Am. **113**, 1166–1176 (2003).

[8] X. Yang and R. O. Cleveland, "Time domain simulation of nonlinear acoustic beams generated by rectangular pistons with application to harmonic imaging," J. Acoust. Soc. Am. **117**, 113–123 (2005).

[9] F. Prieur and S. Holm, "Nonlinear acoustics with fractional loss operators," J. Acoust. Soc. Am. **130**, 1125–1132 (2011).

[10] T. Surguladze, "On certain applications of fractional calculus to viscoelasticity," J. Math. Sci. **112**, 4517–4557 (2002).

[11] Y. A. Rossikhin, "Reflections on two parallel ways in the progress of fractional calculus in mechanics of solids," Appl. Mech. Rev. **63**, 010701 (2010).

[12] J. T. Machado, V. Kiryakova, and F. Mainardi, "Recent history of fractional calculus," Commun. Nonlinear Sci. Numer. Simul. **16**, 1140–1153 (2011).

[13] F. Mainardi, *Fractional Calculus and Waves in Linear Viscoelasticity: An Introduction to Mathematical Models* (Imperial College Press, London, UK, 2010), pp. 1–347.

[14] S. Konjik, L. Oparnica, and D. Zorica, "Waves in fractional Zener type viscoelastic media," J. Math. Anal. Appl. **365**, 259–268 (2010).

[15] M. Caputo, "Linear models of dissipation whose Q is almost frequency independent–II," Geophys. J. Roy. Astr. S. **13**, 529–539 (1967).

[16] R. Weaver and Y. Pao, "Dispersion relations for linear wave propagation in homogeneous and inhomogeneous media," J. Math. Phys. **22**, 1909–1918 (1981).

[17] C. W. Horton, "A loss mechanism for the Pierre shale," Geophysics **24**, 667–680 (1959).

[18] T. Meidav, "Viscoelastic properties of the standard linear solid," Geophys. Prospect. **12**, 1365–2478 (1964).

[19] C. Zener, *Elasticity and Anelasticity of Metals*, (University of Chicago Press, Chicago, 1948), pp. 1–170.

[20] J. J. Markham, R. T. Beyer, and R. B. Lindsay, "Absorption of sound in fluids," Rev. Mod. Phys. **23**, 353–411 (1951).

[21] Y. Rossikhin and M. Shitikova, "Applications of fractional calculus to dynamic problems of linear and nonlinear hereditary mechanics of solids," Appl. Mech. Rev. **50**, 15–67 (1997).

[22] Y. Rossikhin and M. Shitikova, "Application of fractional calculus for dynamic problems of solid mechanics: Novel trends and recent results," Appl. Mech. Rev. **63**, 010801 (2010).

[23] R. L. Bagley and P. J. Torvik, "Fractional calculus—A different approach to the analysis of viscoelastically damped structures," AIAA J. **21**, 741–748 (1983).

[24] D. Craiem, F. Rojo, J. Atienza, G. Guinea, and R. Armentano, "Fractional calculus applied to model arterial viscoelasticity," Latin Am. Appl. Res. **38**, 141–145 (2008).

[25] M. Kohandel, S. Sivaloganathan, G. Tenti, and K. Darvish, "Frequency dependence of complex moduli of brain tissue using a fractional Zener model," Phys. Med. Biol. **50**, 2799–2805 (2005).

[26] G. B. Davis, M. Kohandel, S. Sivaloganathan, and G. Tenti, "The constitutive properties of the brain paraenchyma. Part 2. Fractional derivative approach," Med. Eng. Phys. **28**, 455–459 (2006).

[27] D. Klatt, U. Hamhaber, P. Asbach, J. Braun, and I. Sack, "Noninvasive assessment of the rheological behavior of human organs using multifrequency MR elastography: A study of brain and liver viscoelasticity," Phys. Med. Biol. **52**, 7281–7294 (2007).

[28] I. Sack, B. Beierbach, J. Wuerfel, D. Klatt, U. Hamhaber, S. Papazoglou, P. Martus, and J. Braun, "The impact of aging and gender on brain viscoelasticity," NeuroImage **46**, 652–657 (2009).

[29] M. Caputo and F. Mainardi, "A new dissipation model based on memory mechanism," Pure Appl. Geophys. **91**, 134–147 (1971).

[30] T. Pritz, "Analysis of four-parameter fractional derivative model of real solid materials," J. Sound. Vib. **195**, 103–115 (1996).

[31] T. Pritz, "Five-parameter fractional derivative model for polymeric damping materials," J. Sound. Vib. **265**, 935–952 (2003).

[32] R. Metzler and T. Nonnenmacher, "Fractional relaxation processes and fractional rheological models for the description of a class of viscoelastic materials," Int. J. Plasticity **19**, 941–959 (2003).

[33] T. Pritz, "Loss factor peak of viscoelastic materials: Magnitude to width relations," J. Sound. Vib. **246**, 265–280 (2001).

[34] R. Bagley and P. Torvik, "On the fractional calculus model of viscoelastic behavior," J. Rheol. **30**, 133–155 (1986).

[35] F. Dinzart and P. Lipinski, "Improved five-parameter fractional derivative model for elas tomers," Arch. Mech. **61**, 459–474 (2009).

[36] W. Glöckle and T. Nonnenmacher, "Fractional integral operators and Fox functions in the theory of viscoelasticity," Macromolecules **24**, 6426–6434 (1991).

[37] I. Podlubny, *Fractional Differential Equations* (Academic, New York, 1999), Chap. 1.2.

[38] K. Waters, J. Mobley, and J. Miller, "Causality-imposed (Kramers–-Kronig) relationships between attenuation and dispersion," IEEE Trans. Ultrason. Ferroelectr., Freq. Control **52**, 822–833 (2005).

[39] H. Bass, L. Sutherland, A. Zuckerwar, D. Blackstock, and D. Hester, "Atmospheric absorption of sound: Further developments," J. Acoust. Soc. Am. **97**, 680–683 (1995).

[40] G. Howell and C. Morfey, "Frequency dependence of the speed of sound in air," J. Acoust. Soc. Am. **82**, 375–376 (1987).

[41]H. E. Bass and F. D. Shields, "Ultrasonic relaxation processes," in *Handbook of Acoustics*, edited by M. J. Crocker (Wiley-Interscience, New York, 1998), Chap. 42.

[42]C. Coussot, S. Kalyanam, R. Yapp, and M. Insana, "Fractional derivative models for ultrasonic characterization of polymer and breast tissue viscoelasticity," IEEE Trans. Ultrason. Ferroelectr. Freq. Control **56**, 715–725 (2009).

[43]R. Sinkus, K. Siegmann, T. Xydeas, M. Tanter, C. Claussen, and M. Fink, "MR elastography of breast lesions: Understanding the solid/liquid duality can improve the specificity of contrast- enhanced MR mammography," Magn. Res. Med. **58**, 1135–1144 (2007).

[44]B. E. Treeby and B. T. Cox, "Fast tissue-realistic models of photoacoustic wave propagation for homogeneous attenuating media," Proc. SPIE **7177**, 717716 (2009).

[45]S. Chen, M. Fatemi, and J. F. Greenleaf, "Quantifying elasticity and viscosity from measurement of shear wave speed dispersion," J. Acoust. Soc. Am. **115**, 2781–2785 (2004).

[46]M. W. Urban, M. Fatemi, and J. F. Greenleaf, "Modulation of ultrasound to produce multifre-quency radiation force," J. Acoust. Soc. Am. **127**, 1228–1238 (2010).

[47]S.-E. Måsøy, Ø. Standal, P. Näsholm, T. F. Johansen, R. Hansen, and B. Angelsen, "SURFimaging: In vivo demonstration of an ultrasound contrast agent detection technique," IEEE Trans. Ultrason. Ferroelectr., Freq. Control **55**, 1112–1121 (2008).

[48]S. P. Näsholm, R. Hansen, S.-E. Måsøy, T. F. Johansen, and B. A. J. Angelsen, "Transmit beams adapted to reverberation noise suppression using dual-frequency SURF imaging," IEEE Trans. Ultrason. Ferroelectr., Freq. Control **56**, 2124–2133 (2009).

[49]R. Hansen, S.-E. Måsøy, T. F. Johansen, and B. A. Angelsen, "Utilizing dual frequency band transmit pulse complexes in medical ultrasound imaging., Acoust. Soc. Am. **127**, 579–587 (2010).

[50]K. Papoulia, V. Panoskaltsis, N. Kurup, and I. Korovajchuk, "Rheological representation of fractional order viscoelastic material models," Rheol. Acta **49**, 381–400 (2010).

[51]K. Adolfsson, M. Enelund, and P. Olsson, "On the fractional order model of viscoelasticity," Mech. Time-Dep. Mater. **9**, 15–34 (2005).

[52]A. Chatterjee, "Statistical origins of fractional derivatives in viscoelasticity," J. Sound. Vib. **284**, 1239–1245 (2005).

[53]J. A. T. Machado and A. Galhano, "Fractional dynamics: A statistical perspective," J. Comput. Nonlin. Dynam. **3**, 021201-1 (2008).